Mechatronics 76 (2021) 102550

Contents lists available at ScienceDirect

Mechatronics

journal homepage: www.elsevier.com/locate/mechatronics

A modular low-cost atomic force microscope for precision mechatronics education☆,☆☆

Fangzhou Xia *, James Quigley, Xiaotong Zhang, Chen Yang, Yi Wang, Kamal Youcef-Toumi

Massachusetts Institute of Technology Mechatronics Research Lab: 77 Massachusetts Avenue, Room 1-010, Cambridge, MA, 02139, United States of America

ARTICLE INFO

Keywords:
Atomic Force Microscope
Active cantilever probe
Modular low-cost system
Precision mechatronics
Piezo scanner design
Education

ABSTRACT

Precision mechatronics and nanotechnology communities can both benefit from a course centered around an Atomic Force Microscope (AFM). Developing an AFM can provide precision mechatronics engineers with a valuable multidisciplinary hands-on training experience. In return, such expertise can be applied to the design and implementation of new precision instruments, which helps nanotechnology researchers make new scientific discoveries. However, existing AFMs are not suitable for mechatronics education due to their different original design intentions. Therefore, we address this challenge by developing an AFM intended for precision mechatronics education.

This paper presents the design and implementation of an educational AFM and its corresponding precision mechatronics class. The modular educational AFM is low-cost (≤ $4,000) and easy to operate. The cost reduction is enabled by new subsystem development of a buzzer-actuated scanner and demodulation electronics designed to interface with a myRIO data acquisition system. Moreover, the use of an active cantilever probe with piezoresistive sensing and thermomechanical actuation significantly reduced experiment setup overhead with improved operational safety. In the end, the developed AFM capabilities are demonstrated with imaging results. The paper also showcases the course design centered around selected subsystems. The new AFM design allows scientific-method-based learning, maximizes utilization of existing resources, and offers potential subsystem upgrades for high-end research applications. The presented instrument and course can help connect members of both the AFM and the mechatronics communities to further develop advanced techniques for new applications.

1. Introduction

An Atomic Force Microscope (AFM) can be a great platform for precision mechatronics education. The AFM is a versatile instrument for nanoscale surface characterization widely used in physics, chemistry, biology and material science. The development of an AFM involves various subsystems suitable for teaching mechatronic concepts through hands-on experiments. Multidisciplinary topics can be taught by developing a nano-positioner for mechanical design, a piezo actuator driver for electrical circuits, a cantilever oscillation demodulator for signal processing, a probe deflection regulator for dynamic system control and user interface software for programming. As a result, students can practice precision mechatronic techniques comprehensively by developing a functional AFM for nanoscale imaging throughout a semester.

The scanning probe microscope (SPM) community can also benefit significantly from precision mechatronics education centered around AFMs. On one hand, researchers need to modify AFMs to enable functionalities that are required in new applications. For example, adding an infrared source for tip-enhanced scanning near-field optical microscopy (SNOM) allows material property mapping with high resolution to overcome the diffraction limitation [1]. Such modification requires knowledge of mechatronics typically beyond regular AFM users, who are mostly nanotechnology researchers. Hence, studying AFM from a mechatronics perspective empowers researchers to develop customized new AFM capabilities. On the other hand, mechatronic engineers who are familiar with AFMs can help improve its performance. For instance, video-rate AFM have been developed for dynamic chemical reaction process visualization [2,3]. This is realized with customized mechatronic system design including high-speed scanners [4,5], high-bandwidth power amplifiers [6], control algorithms [7], etc.

☆ Acknowledgment: The authors are grateful for the financial and technical support provided by Synfuels Americas, United States of America. The authors also acknowledge the hardware and software support by nano analytik GmbH and National Instruments.

☆☆ This paper was recommended for publication by Associate Editor Tom Oomen.

* Corresponding author.
E-mail addresses: xiafz@mit.edu, xiafz@umich.edu (F. Xia).

https://doi.org/10.1016/j.mechatronics.2021.102550
Received 19 October 2020; Received in revised form 5 February 2021; Accepted 14 March 2021
Available online 13 April 2021

Therefore, AFM based precision mechatronics education can help cultivate both researchers and engineers for the SPM community. In fact, such techniques can be broadly applied in developing other precision instruments. These, in turn, will allow researchers to make new scientific discoveries and assist in meeting the increasing demands in nanotechnology.

AFMs have not been widely used for precision mechatronics education mainly due to the lack of a suitable platform. A commercial AFM typically costs beyond $30,000, which is too expensive to be taken apart in a mechatronics class. Moreover, the non-modular design also makes it difficult to customize subsystems. As an alternative, current AFM classes either focus on physical principle modeling [8] or provide training sessions using research AFMs for imaging experiments. Since mechatronics education require significant hands-on experience working with various subsystems, it is difficult to use expensive and non-modular AFMs for teaching. In this work, we address this challenge by developing a modular low-cost ($\lesssim$ $4000) and easy-to-operate AFM suitable for precision mechatronics education.

The paper is organized as follows. First, we provide an overview of educational AFM design principles with benchmarks from existing systems. The aspects of improvement and comparative advantages of the proposed system are emphasized. Second, design and analysis of primary subsystems are discussed for the cantilever probe, nanopositioner and electronics. With constrained resources, a number of new strategies are evaluated and optimized for this AFM during system design and integration. Third, experimental results and performance analysis of a prototype AFM are presented and discussed. Finally, we conclude this work with a graduate-level full-semester AFM course design.

2. Educational AFM design principles

The design of an AFM for mechatronics education has special requirements. The primary aspects to consider include affordability, modularity, ease of operation and compatibility for educational experiments. First, the design needs to fit within the hardware purchase budget limitation of typical lab-based university classes around hundreds of dollars per student. Second, a modular design with decoupled subsystems is needed to reduce debugging complexity and ensure a functional final assembly. It also allows potential upgrades of system capabilities for more advanced imaging applications. Third, the educational AFM should be easy to operate so that students can focus on the mechatronic development. Specifically, the cantilever installation and imaging experiment preparation should be improved to reduce the setup time and minimize the risk of damaging the system. Fourth, each AFM subsystem should have compatible experiments for students to practice precision mechatronic design and verify fundamental theoretical models. If these requirements are satisfied, the AFM platform can be suitable for precision mechatronics education.

2.1. Benchmark systems

Existing commercialized educational AFMs are designed for imaging demonstrations instead of mechatronics education. A comparison of six commercial educational AFMs based on the four aforementioned criteria are summarized in Table 1, which is ranked in a cost descending order (2019 quotes). AFMs for in-class imaging demonstrations usually have a packaged design for portability, which yields a low level of modularity needed for mechatronic system design experiments. The top four conventional designs listed in Table 1 use optical beam deflection (OBD) sensing for passive AFM cantilever probes. They are more expensive and require probe-laser alignment for experiment setup. The nGauge AFM from ICSPI and the proposed design uses active AFM cantilever probes with embedded sensing and actuation that are easier to operate. The scanner is also miniaturized using Microelectromechanical systems (MEMS) technology. With its portability, this design is perfect for AFM imaging demonstration but not as much for precision mechaotrnics education since most components are produced with nanofabrication. For the Stromlingo Nssembly AFM, an Optical Pickup Unit (OPU) in a DVD-drive is repurposed to measure the AFM cantilever deflection [9]. In terms of price and modularity, this design is appealing for mechatronics education as it offers Do-It-Yourself (DIY) assembly at a very low cost. However, this system is currently limited to contact mode imaging in ambient air only. Moreover, the close proximity requirement of the OPU and the cantilever introduces extra alignment complexity.

By comparison, the AFM design in this work has the lowest cost with modular design suitable for education of precision mechatronic system development. It is also easier and safer to operate for imaging experiments by removing the need for probe-laser alignment and reducing actuator operating voltage. In addition to commercial education systems, a macroscopic AFM have been successfully developed for precision mechatronics education purpose with a relatively more expensive data acquisition system [10]. The system developed in this work takes a step further to realize true nanoscale AFM imaging with a lower cost by using the NI myRIO data acquisition system.

3. Low-cost AFM primary subsystem design

In this section, four important subsystems and their integration for the modular low-cost AFM are discussed. They are the active cantilever probe, the signal processing electronics, the scanner with drivers, and the software interface. The modular decoupled subsystems can be individually debugged before integration into the final system with the overall design and bill of materials available at the end of this section.

3.1. Active cantilever probe

In contrast to a passive probe, an active AFM probe contains embedded sensors and actuators. Conventional AFMs use passive probes with a base silicon chip, a micro-cantilever and a sharp tip. For sensing, the OBD system achieves sub-nanometer resolution by using an optical level to amplify and measure the cantilever deflection, and a quadrature photodiode. In terms of actuation, piezoelectric actuators are used to excite the resonance of the probe with acoustic vibration propagation though the probe holder structure. As an alternative, active probes have nanofabricated functional electronics on the cantilever to realize deflection sensing and actuation without external bulky components.

Using passive AFM probes for imaging requires significant operator experience. Specifically, users need to manually handle the small probe base chip (typically 3.4 mm long, 1.6 mm wide, and 0.3 mm thick), properly align the laser and cantilever (tens of microns), identify the cantilever resonance in tapping mode while avoiding spurious structure resonance [11], etc. Consequently, such operational complexity increases the overhead and risk of equipment damage when handled by novice users. Moreover, the laser and optical components are fragile and relatively expensive to repair.

Active probes are preferred over passive probes for education purposes. They resolve the aforementioned issues by changing the fundamental principles of deflection sensing and actuation. Without the laser sensing system, active probes can remove the operation overhead for alignment, lower the risk of manual error and reduce the cost of optical components. For resonance excitation, embedded actuators in active probes do not excite the structure resonance, which makes tapping mode imaging experiment much easier.

The functional elements of the active probe used in this work are shown in Fig. 1(a). This probe has an embedded piezoresistive deflection sensor and a bimorph structure thermomechanical actuator. In its basic form, this probe design can be used for contact and tapping mode imaging in air. The active probe imaging performance is comparable to conventional passive AFM probes. By applying a proper coating layer, it is also possible to conduct imaging in specialized opaque

Table 1
Comparison of commercialized AFM systems and the proposed AFM based on educational system design principles.

AFM System & Vendor	Cost ($)	Modularity	Probe operation principle	Experiment
Nanosurf Naio	27,900	Packaged portable	Optical beam deflection	Imaging demonstration
Nanomagnetics ezAFM	22,000	Packaged portable	Optical beam deflection	Imaging demonstration
AFM Workshop B-AFM	19,495	Modular	Optical beam deflection	Mechatronics design
Thorlabs Educational	13,145	Modular	Optical beam deflection	Mechatronics design
ICSPI nGauge	7,000	Packaged portable	MEMS scanner active	Imaging demonstration
Stromlingo Nssembly	5,000	Special DIY assembly	Optical pick-up unit	DIY assembly
Design in this work	4,000	Modular	Piezoresistive bimorph	Mechatronics design

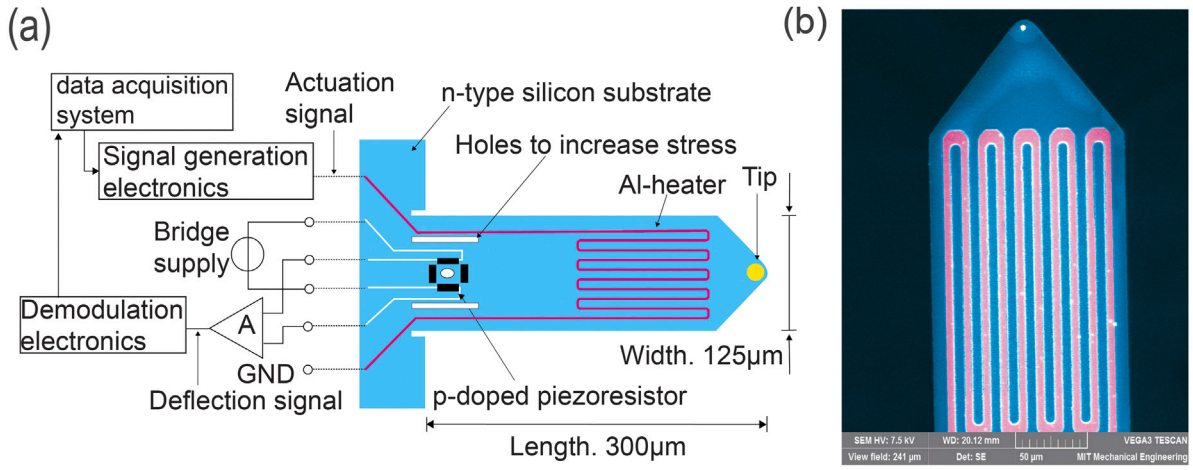

Fig. 1. Active cantilever probe: (a) dimension illustration with subsystem labels, (b) colored SEM image of the aluminum heating wires (the piezoresistive sensing elements covered by protective epoxy at the base are not shown).

liquid environments [12]. Superior capabilities can be achieved by using active probes with specialized functionalization. For example, with a conductive tip, scanning probe lithography can be enabled to achieve sub-nanometer resolution pattern generation and imaging [13]. In terms of imaging speed, up to 200 lines per second has been realized [14]. Moreover, by integrating four cantilevers in parallel, high-throughput large-area inspection with image stitching can be achieved [15]. The authors have years of experience realizing and extending AFM capabilities by designing systems centered around this active probe with various applications summarized in this review [16].

For deflection sensing, piezoresistors are used to measure the cantilever internal stress, which is proportional to the deflection. Four P-doped silicon piezoresistive elements are placed on the top surface at the cantilever fixed end, where the internal stress is maximized. A full Wheatstone bridge circuit is used to measured the piezoresistor resistance variation to compensate for the thermal drift. The governing relations for the voltage output U_{out} and the resistive Johnson noise floor z_{noise} are shown in Eq. (1) for a cantilever with length ℓ, width w, and thickness h. In Eq. (1), U_b is the bridge supply voltage, F is the force applied at the cantilever free end, z is the cantilever deflection, P_R is the sensor piezoresistive coefficient, E is the effective elastic modulus of the cantilever, k_B is the Boltzmann constant, R is the nominal resistance of each piezoresistive element, and B is the measurement bandwidth.

$$U_{out} = \frac{6P_R F}{wh^2}U_b = \frac{3P_R hEz}{\ell^2}U_b, \quad \Delta z_{noise} = \frac{4\ell^2\sqrt{4k_B TRB}}{3EP_R hU_b} \tag{1}$$

For excitation of the cantilever resonance, a nanofabricated bimorph structure composed of a silicon layer and a silicon nitride layer is used with an aluminum heating wire. Both the dynamic oscillation and the static defection of the cantilever can be controlled using the heating element [17] with governing equation in Eq. (2).

$$z_t = 3K\Delta T\ell^2, \text{ with } K \triangleq \frac{3(\alpha_2-\alpha_1)(h_1+h_2)}{h_2^2\left[3\left(1+\frac{h_1}{h_2}\right)^2+\left(1+\frac{h_1E_1}{h_2E_2}\right)\left(\frac{h_1^2}{h_2^2}+\frac{h_2E_2}{h_1E_1}\right)\right]} \tag{2}$$

where z_t is the cantilever tip deflection, α_1 and α_2 are the coefficients of thermal expansion, h_1 and h_2 are the thicknesses for the silicon and silicon nitride layers, E_1 and E_2 are the corresponding elastic moduli, ℓ is the cantilever length, and ΔT is the temperature difference between the heated cantilever and room temperature. A summary of the physical principles is shown in Fig. 2(a) with more detailed derivations in [18,19].

In terms of packaging, the active cantilever probe is bounded onto a PCB with micro SD-card-Shape for ease of manual handling. An optical microscope image of the bounded cantilever is shown in Fig. 2(b). The plug-and-play operation without laser alignment makes it more user friendly compared to passive probes. Lead wire connections with electrical protection allow direct interface to signal conditioning circuits.

A number of physical principles can be used for AFM cantilever deflection sensing and resonance excitation. A summary of these principles is provided in Table 2. The review includes function (sensing or actuation), signal type (DC or AC), transducer size (bulk or embedded), main limitation, availability, and references to the corresponding research. Active probes combine embedded principles to achieve cantilever deflection sensing and actuation. With the advancement of MEMS technology, accessibility to active probes has been improved greatly in the last decade.

Several relatively matured active probe designs have been commercialized. The first example is active probes using the quartz tuning fork including the qPlus sensor [20] available at NaugaNeedles and the Akiyama probe [21] commercialized by NanoSensors. This probe

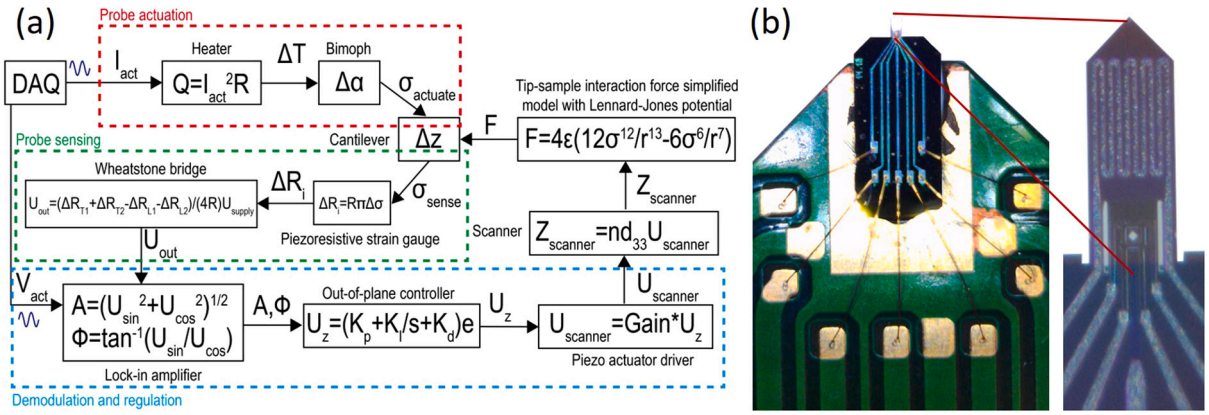

Fig. 2. Active probe AFM principles: (a) physical principle illustration with signal paths, (b) optical microscope image of the active cantilever bounded on a PCB with SD-card-shape geometry and zoomed in view of the functional elements.

utilizes the piezoelectric effect of the tuning fork for both sensing and actuation, which works even in cryogenic environment. However, due to the charge leakage problem, this design is only suitable for tapping mode operation. The system dynamics is also relatively more complicated since both the tuning fork and the microcantilever can have multiple resonance modes. A piezoresistive self-sensing probe has also been commercialized by SCL SensorTech. This design can operate in both contact and tapping modes but requires external piezoacoustic actuation for resonance excitation. The piezoresistive sensing thermomechanical actuation probe selected in this work has been commercialized by nano Analytik GmbH. This probe can be used in both contact and tapping modes and even offers static deflection control. One minor disadvantage is its sensitivity to temperature variation and thus room-temperature operation is desired. As introduced in the benchmark systems section, the nGauge active probe AFM from ICSPI also utilize a piezoresistive sensing cantilever with vertical and horizontal MEMS actuators for scanning.

In a mechatronics educational scenario, the selected active probe is easy to operate and cost effective. By inserting the SD-card-shape probe into the slots of the pre-amplification PCB, students can readily conduct frequency sweeps and verify the deflection signal of the probe using an oscilloscope. This significantly reduces the chance of probe damage due to improper handling. Students as novice AFM users feel more comfortable to handle this probe and spend less time debugging the deflection sensing system. For AFM development in a mechatronics class, it is worth to note that the cantilevers are broken more often due to manual handling than tip wear during relatively infrequent imaging experiments. Moreover, when used in tapping mode, cantilevers can last even longer with the small tip-sample interaction force. Experience in the lab shows that active probes last significantly longer than passive probes. During experiments, students often break passive cantilever as they manually handle the small probes. Although the unit cost of each active probe is around five times that of standard passive probes, it can be more cost effective for precision mechatronics lab sessions.

In summary, the active probe selected is suitable for the educational AFM. The probes have good functionality and a wide range of established research applications. It is also commercially available, easy to operate and cost effective.

3.2. Tapping mode signal processing electronics

Specialized signal processing electronics need to be designed for AFM tapping mode imaging. As a well-known advantage, tapping mode reduces tip-sample friction force. Moreover, there is a smaller probe damage risk due to improperly tuned controller compared to contact mode since the cantilever is not always being deflected. Instead of the static deflection, the amplitude or the phase of the cantilever oscillation can be regulated in tapping mode.

Two main challenges for tapping mode signal processing in this design include the relatively low DAQ sampling rate and clock synchronization. The first resonance frequency of the active cantilever probe is typically between 20 kHz to 100 kHz. As the price of high-end DAQs are beyond the budget limit, the selected affordable myRIO-1900 digital to analog converters (DAC) and analog to digital converters (ADC) have limited sampling frequencies at 345 kHz and 500 kHz. As a result, the DDC/ADC sampling rates are insufficient for direct digital probe excitation and demodulation. Therefore, custom electronics are designed to pre-process the signal to reduce the required sampling frequency. Moreover, the custom designed signal generation and the demodulation circuits need to be synchronized to avoid inaccuracies due to clock mismatch. The signal processing circuit function diagram is shown in Fig. 3(a) with implementation in Fig. 3(b).

For resonance excitation, an AD9833 integrated circuit (IC) is used to generate the sine wave with direct digital synthesis. To ensure clock synchronization, a 20 MHz square wave generated by the myRIO digital output line provides a reference clock to the AD9833. The desired frequency and phase are specified with serial peripheral interface (SPI) communication. The generated sine wave has valleys and peaks between 38 mV and 650 mV. The signal is then passed through a non-inverting amplifier buffer and a non-inverting voltage adder with variable gain to scale the output voltage. The voltage adder also uses the myRIO analog output signal to adjust the DC offset before driving the heater. For thermomechanical actuation, the heat power P_{heat} is proportional to the square of the input voltage. By using trigonometric identities, a harmonic at twice the input signal frequency arises as derived in Eq. (3).

$$P_{heat} = \frac{1}{R}\left[V_{dc}^2 + 2V_{dc}V_{ac}\sin(\omega t) + \frac{1}{2}V_{ac}^2(1-\cos(2\omega t))\right] \tag{3}$$

If no static offset control is needed, the active probe is driven by providing a zero offset V_{dc} and applying a sinusoidal voltage signal $V_{ac}\sin(\omega t)$ at half of the frequency of the cantilever resonance. For education purpose, the excitation circuit design essentially constructed a simple functional generator, which can be offered as a lab module for student practice.

For oscillation demodulation, a number of techniques are available. Depending on whether the demodulation is synchronous or not, they can generally be classified as rectification and mixing [34]. Rectification methods such as the moving average filter and peak detectors are easy to implement but assumes the sinusoidal signal being demodulated is not mixed with other signals. The presence of noise or signals at other frequencies will affect its demodulation performance. With the potential presence of two harmonics and DC signal from the thermomechanical actuation, rectification demodulation methods are not suitable. Mixing methods such as the lock-in amplifier, the Kalman filter and the Lyapunov filter offer very good off-frequency noise rejection

Table 2
Cantilever sensing and actuation principle comparison summary with reference to representative research.

Physical principle	Function	Signal	Footprint	Main limitation	Availability	Reference
Optical beam deflection	Sensing	DC&AC	Bulk	Transparency	Commercial	[22]
Astigmatic detection	Sensing	DC&AC	Bulk	Transparency	Commercial	[23]
Interferometry	Sensing	DC&AC	Bulk	Transparency	Commercial	[24,25]
Optomechanical	Sensing	DC&AC	Embedded	Transparency	Research	[26]
Piezoresistive	Sensing	DC&AC	Embedded	Thermal noise	Commercial	[27]
Piezoelectric	Both	AC only	Embedded	Charge leakage	Commercial	[20,21]
Piezoacoustic	Actuation	AC only	Bulk	Structure vibration	Commercial	[28]
Photothermal	Actuation	DC&AC	Bulk	Thermal sensitivity	Commercial	[29]
Thermomechanical	Actuation	DC&AC	Embedded	Thermal sensitivity	Commercial	[30]
Electromagnetic	Actuation	DC&AC	Bulk	Magnetic sample	Research	[31]
Electrostatic	Actuation	DC&AC	Bulk	Sample capacitance	Research	[32,33]

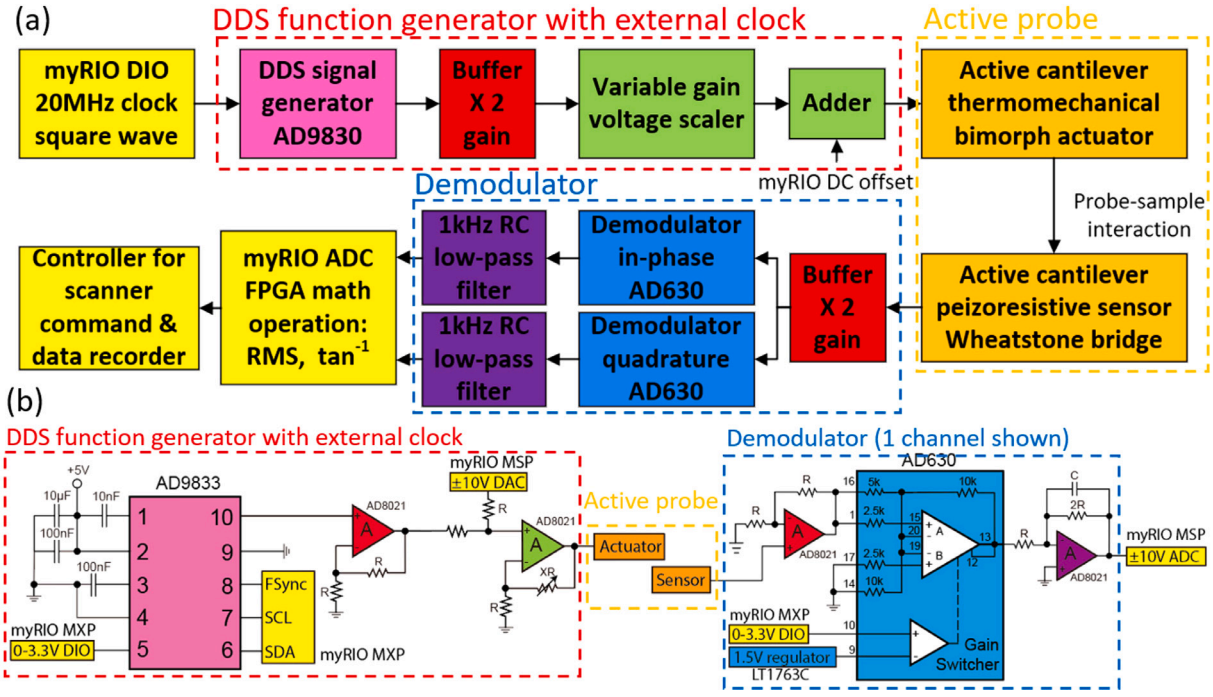

Fig. 3. Signal processing circuit: (a) functional diagram of the signal generation and demodulation process, (b) schematic of an AD9833 direct digital synthesis function generator and a single AD630 demodulator channel.

by using a reference signal but are relatively more complicated to implement. Digital lock-in amplifiers are the most widely used demodulation method for tapping mode AFM with its good performance, commercial availability and relatively straightforward implementation. In principle, digital lock-in amplifiers can be directly implemented on Field Programmable Gate Array (FPGA) for AFM cantilever oscillation demodulation. For example, a high-end NI PXIe-7975R FPGA with an NI5782 ADC/DAC running at 250 MHz sampling rate was used to implement a digital lock-in amplifier in previous work [12]. Directly implementing this digital lock-in amplifier on the myRIO DAQ system is not feasible due to the low sampling rate and the limited space available on the myRIO FPGA. Therefore, an analog frequency mixer is designed to remove the need for high sampling rate and reduce the required FPGA computational resources.

In this work, two AD630 IC chips are configured as a lock-in amplifier for synchronous demodulation. Each AD630 is a variable gain amplifier with ± 2 gain where the sign of the gain is controlled by the myRIO digital lines with a square wave at the cantilever resonance frequency. A low-pass filter at 1 kHz is used to extract the envelope. If two channels of the demodulator with square wave input signals having a phase offset by 90° are used to obtain signals z_{cos} and z_{sin}, both the amplitude and the phase can be computed with the lock-in amplification formula as in Eq. (4). This PCB design task is a great opportunity for students to practice their circuit instrumentation skills.

$$A(t) = 2\sqrt{z_{cos}^2 + z_{sin}^2}, \quad \phi(t) = \arctan\left(\frac{z_{sin}}{z_{cos}}\right) \tag{4}$$

3.3. Piezo buzzer scanner

The scanner design is based on piezo buzzers. Since piezo buzzers are low-cost and work at relatively low voltages, they can be safely handled by students for custom designs during trial and error. In contrast, conventional AFM scanners with stacked piezo actuators or piezo tubes require high-voltage drivers that can be both expensive and dangerous. Most buzzers are round and have a sandwich structure with a copper disk, a piezoelectric layer and a silver electrode. Buzzers for speakers typically have diameters between 10 mm to 40 mm and unloaded resonance frequencies between 2 kHz to 12 kHz. The voltage-controlled expansion and contraction of the piezoelectric material in the radial direction results in an amplified motion perpendicular to the disk. A center deformation gain of 150 nm/V is typical for most buzzers. A rated voltage of 30 V would result in a motion range around 4.5 μm. Higher voltage can also be applied to increase the motion range for low frequency driving signals. In this work, a multi-actuated buzzer AFM scanner design formed by stacking two different configurations is used. The overall geometric configuration of the scanner is shown in Fig. 4 with parameter labels and motion principle illustration.

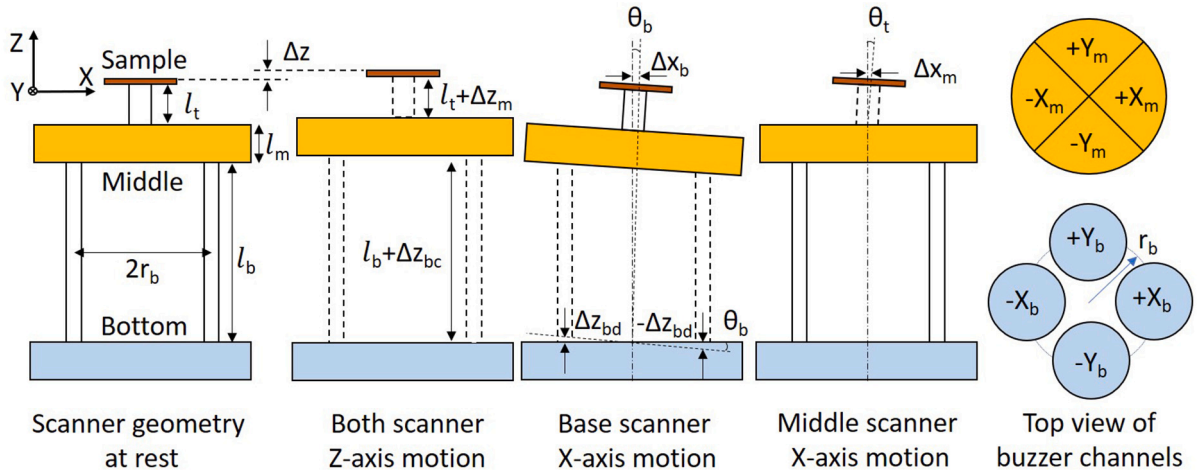

Fig. 4. Multi-actuated buzzer scanner design with variable definitions, motion principle illustration for both out-of-plane and in-plane directions and top view of the single buzzer four quadrant middle scanner and four buzzer bottom scanner.

The bottom scanner is composed of four buzzers with 15 mm diameter positioned evenly around a circle with radius $r_b = 11.5$ mm. Four aluminum rods with length $l_b = 1.5$ in. and 0.125 in. diameter are used to connect the bottom layer to the middle layer. For the middle scanner, a 30 mm diameter large buzzer is used with its electrode evenly divided into four quadrants. A magnetic pillar with length $l_t = 0.375$ in. and 0.3125 in. diameter is glued to the center of the large buzzer. The sample puck is magnetically attached on top of the magnetic pillar. The scanner structure is 3D printed for cost-efficiency and ease of fabrication. Using metal structures can improve the dynamic performance.

The out-of-plane motion Δz is obtained from the sum of both the bottom buzzers Δz_b and the middle buzzer Δz_m as $\Delta_z = \Delta z_b + \Delta z_m$. The X direction in-plane motion of the sample $\Delta x = \Delta x_b + \Delta x_m$ have contributions from both the small buzzers at the bottom x_b and the large buzzer in the center x_m as summarized in Eq. (5).

$$\Delta x_b = (l_b + l_m + l_t)\sin\theta_b \approx (l_b + l_m + l_t)\frac{\Delta z_b}{r_b}, \quad \Delta x_m = l_t \sin\theta_m \tag{5}$$

In addition to the previously defined dimensions, l_c denotes the spacing between the top of the aluminum rode and the bottom of magnetic pillar. For the four buzzer configuration, the small angle approximation $\sin\theta_b \approx \theta_b$ is applied to relate θ_b to the geometric quantities. The angle θ_m of the middle buzzer is difficult to express analytically but is proportional to the applied voltage. The motion equations in the Y direction is similar to the X direction.

The performance of the scanner is verified with a SIOS SP-120 laser interferometer. With ±30 V driving voltage, the bottom buzzers produce 16 μm square in-plane range and 3.75 μm out-of-plane range. The middle buzzer produces 2.5 μm square in-plane range and 8 μm out-of-plane range. Due to imperfect alignment, motion coupling between the out-of-plane and the in-plane axes are around 1.25% to 1.75%. An in-plane coupling at around 3% between the X and the Y axis is observed. The in-plane bandwidth of the scanner is around 75 Hz, which is sufficient for AFM imaging.

3.4. Piezo buzzer driver

This subsection discuss the piezo buzzer driver design. The driver has six inputs from myRIO-1900 and eight outputs to the buzzer elements as shown in Fig. 5(a). Four DACs with 0–5 V range on the myRIO MXP connector are used to control the in-plane motions for both the bottom buzzers and middle buzzer. Two myRIO MSP connector ±10 V DACs are used for the out-of-plane motion. Multiple OPA445 operational amplifiers are used to drive the buzzer scanner.

To drive the scanner, the 2.5 V offset of the in-plane voltage command 0–5 V is removed and amplified to ±10 V range. The signal is duplicated with an inverter to produce differential drive signals to the two opposing buzzers for in-plane scanning. The ±10 V voltage signal for the Z axis command is then added to both signals from the differential drive stage and amplified by a gain of 3 to drive the buzzers.

It is evident from the driving principle that the maximum range of the in-plane motion and the out-of plane motion for the same set of buzzers cannot be realized simultaneously due to the voltage limitation. With a fixed DAC resolution, a smaller scanning range yields a higher positioning accuracy. The multi-actuated scanner design provides more flexibility in operation for scanning with different range and resolution. The bottom four buzzers offer a larger in-plane range but a smaller out-of-plane range compared to the middle buzzer with four quadrants.

3.5. Software interface

The myRIO microcontroller is selected for its wide availability in academic institutions. It is easy to program using graphical LabVIEW software, which allows students to focus on control algorithm development rather than code debugging. The low-level Proportional–Derivative–Integrator (PID) controller for closed loop AFM operation are implemented on the FPGA with hardware interfacing. An event-driven state machine structure with five states including idle, engaging, engaged, scanning, and retract are implemented on the real-time system for user input handling and data recording. The overall software implementation is based on the code developed previously on an NI FlexRIO system for a high-end AFM system in the lab [12], which is optimized to work on NI myRIO.

3.6. System integration

The overall CAD design with color-coded subsystem labels of the educational AFM system is shown in Fig. 6(a). In addition to the primary subsystems introduced above, several additional components are needed. For coarse positioning, a DS40-XYZ dovetail linear stage is used to achieve 0.55 in square in-plane range and 0.25 in out-of-plane range. The in-plane directions are adjusted manually for coarse sample positioning. The out-of-plane direction is driven by a Nema 11 stepper motor with 100 : 1 gear reduction from StepperOnline together with a DM320T stepper driver. An Opti-Tekscope digital microscope with 200x zoom and 1600 by 1200 pixel resolution provides an optical view. The connection between various electrical components of the AFM is shown in Fig. 6(b).

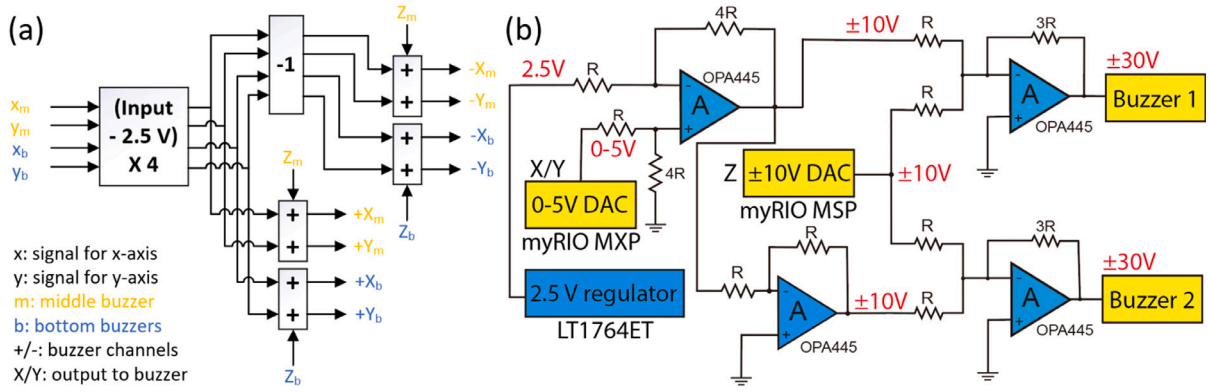

Fig. 5. Electrical system configuration: (a) functional diagram of the multi-channel driver circuit for interface between myRIO microcontroller and the scanner, (b) signal channel driver circuit schematic.

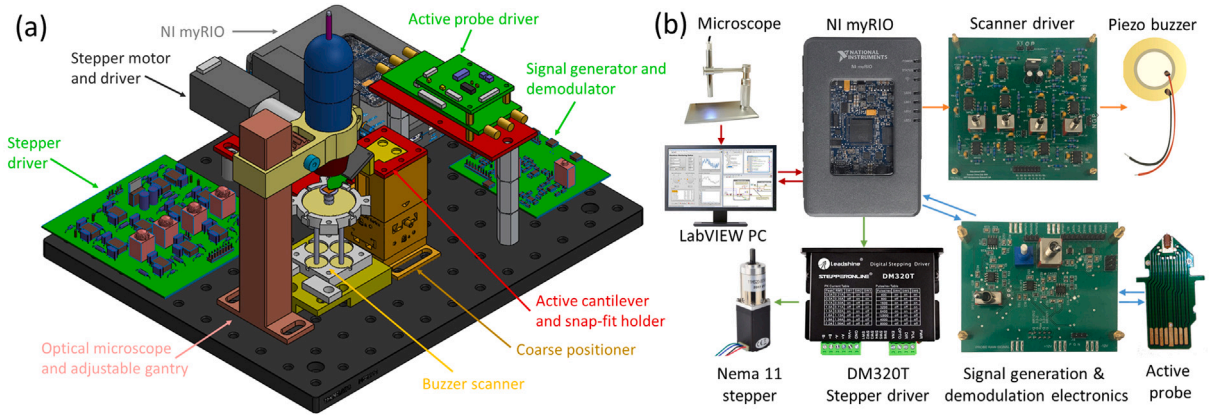

Fig. 6. System integration and experiment results: (a) CAD design with color-coded subsystem labels, (b) custom electronics design centered around NI myRIO for AFM data acquisition.

The overall bill of materials is provided below for each primary subsystem with estimated pricing based on purchase made by the authors in the US. The specific prices may change depending on the source of purchase.

Course positioning and engagement system: (a) Nema 11 Stepper Motor with 100 gear reduction ($41.75), (b) bracket mount for the stepper motor ($5.66), (c) DS40-XYZ positioning stage ($435), (d) shaft coupler ($3).

Buzzer scanner: (a) piezoelectric buzzers (< $20), (b) 3D printing structure materials

Electronic components: (a) buzzer scanner driver PCB (< $100), (b) demodulation and signal generation PCB (< $120), (c) AC to DC power converter (< $150), (d) probe driver circuit ($400), (e) active cantilever probe: ($130)

Mechanical components: (a) optical breadboard ($134.64), (b) sorbothane sheet ($28.95), (c) fixtures (<$50)

Shared components: (a) NI myRIO 1900 ($567), (b) Opti-Tekscope microscope: ($69.95)

In summary, the total cost of the AFM with 3 active probes is below $4000 with the fixed cost below $3000. For the custom designed PCBs and scanners, a $1000 per system variable cost would be sufficient for recurring class offering.

4. Results and discussion

In this section, we provide the experimental imaging results and analyze the performance of the educational AFM. A picture of the assembled prototype of an educational AFM system is shown in Fig. 7(a).

4.1. Imaging experiments

To verify the imaging capability of the low-cost educational AFM system, we took images of a TG-XYZ03 calibration sample with 500 ± 15 nm feature depth in the 5±0.1 μm pitch area with square pits. During the imaging, the bottom buzzers are used for in-plane scanning across a 15 μm by 15 μm range at two lines per second and the middle buzzer is used for out-of-plane topography tracking. The imaging result is shown in Fig. 7(b). With the tilting angle of 15° of the probe, the bottom of the pits is a bit distorted. This is potentially due to the probe oscillation being affected by the edge of the pits rather than reaching the bottom and the "parachuting effect" of the controller when encountering a sudden step-down in the topography. Nevertheless, the imaging capability of the system is demonstrated.

A TGZ-100 calibration grating is imaged for further evaluation of the AFM resolution capability. The sample has smaller feature size with 110 ± 2 nm height and 3 ± 0.01 μm pitch. The image is taken using similar scanning settings at a range of 13 μm by 13 μm. As shown in 7(c), the features can still be successfully resolved by the educational AFM prototype. We did notice certain non-linearity for the in-plane scanning direction due to the non-ideal manual assembly of the simple buzzer scanner. This problem is not crucial during mechatronics education for demonstration of the overall functionality and can be compensated in the post-processing stage if needed.

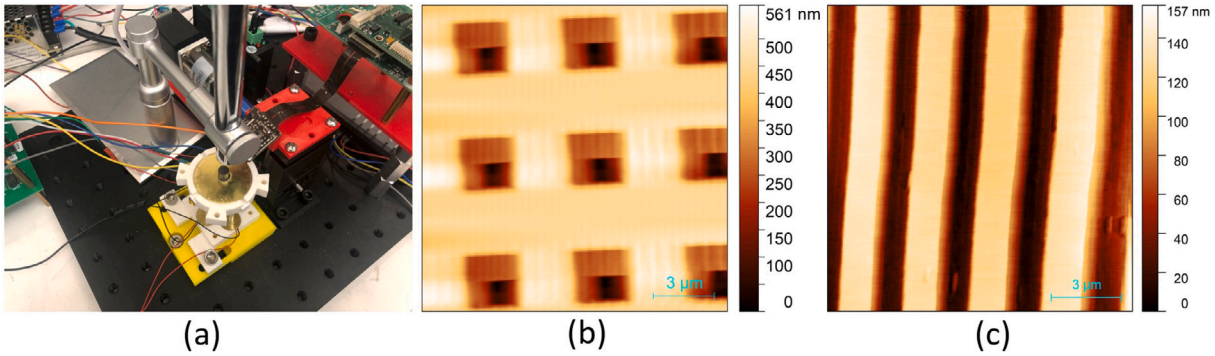

Fig. 7. System integration and experiment results: (a) image of the assembled AFM system with electronics and an optical microscope, (b) 15 μm by 15 μm image taken for the 5 ± 0.1 μm pitch square-pit area of a TGXYZ03 calibration grating (NanoAndMore) with 500 ± 15 nm, (c) 13 μm by 13 μm image taken for a TGZ-100 calibration grating (Ted Pella) with trances of 110 ± 2 nm height and 3 ± 0.01 μm pitch.

4.2. Performance analysis

The performance of the educational AFM is mostly determined by the scanner and the data acquisition system. The developed system can achieve nanometer resolution with a scan speed of two lines per second, which is sufficient for most imaging purposes. Achieving sub-nanometer resolution as high-end commercial systems can be challenging as limited by the low-cost buzzer scanner and the myRIO DAQ system. With a 12-bit DAC resolution and an overall 11.75 μm out-of-plane positioning range, the quantization error would limit the scanner resolution be around 3 nm. The in-plane total range of 18.5 μm would also yield close to 5 nm positioning uncertainty. With additional noise from the environment, the noise floor of the educational AFM is observed to be around 6 nm. By using commercial piezo scanners and high-end DAQ systems, better resolution performance can be achieved since the active probe is not the limiting factor. The noise performance can also be improved by replacing the sorbothane sheet with a pneumatic suspension optical table. The authors have proven the possibility of high-end AFM capabilities with previous work for various applications where cost reduction is not the primary consideration [12,16]. Indeed, with the modularity of this design, researchers are encouraged to modify the AFM with higher-end nano-positioners and DAQ systems for research grade applications.

5. AFM platform experiments and educational impacts

A graduate-level full-semester course is designed around the low-cost educational AFM. The class provides a unified framework for multidisciplinary education with in-depth hands-on learning. A total of twenty-five lectures cover five general topics including precision mechatronic system principles, control systems, AFM system design, advanced applications and related fields. Important AFM subsystems such as active cantilevers, positioners, and electronics are used as design examples. Students practice lecture theories extensively through lab experiments with selected lab topics listed below.

1. AFM Cantilever: piezoresistive deflection sensitivity calibration, probe frequency response identification, cantilever stiffness measurement, thermomechanical actuation model verification as in Eq. (2).
2. Positioning Systems: LabVIEW stepper motor control, piezo buzzer scanner design (Section 3.3), scanner range and bandwidth characterization with laser interferometer, flexure-based AFM scanner design with FEA simulation
3. Electronics & circuit design: signal generation and demodulation (Section 3.2), piezo buzzer driver
4. Imaging: AFM imaging of selected samples, AFM image data post-processing with Gwyddion
5. Investigation: LabVIEW control/simulation exercises, feedforward AFM imaging algorithm implementation, cantilever nanofabrication, micro/nano sensor instrumentation, motion control algorithms, FPGA sigma-delta modulation, unconventional AFM imaging mode development (e.g. contact resonance), etc.

Centered around the subsystems, students are given the opportunities to practice precision mechatronic system design and implementation skills. Students can also verify the models developed in the lecture to better appreciate the benefits of mathematical analysis to speed-up the design process. The practical experience enables the students to conduct further research on imaging instruments and complex mechatronic systems. The course design also helps to cultivate a community of AFM users and developers across multiple departments in the institution that can initiate potential collaborations. A pilot study for an abbreviated version of the class covering the first module through five lectures and four hands-on labs have been offered in January 2020 at MIT during the winter break as a workshop. The content was well received among the 40 registered participants from various disciplines including both engineers with mechatronic system development experience and regular AFM users conducting nanotechnology research.

6. Conclusion and future work

In this work, we designed and implemented a low-cost AFM system for educational purpose by utilizing the active cantilever probe technology. With cost and performance consideration in mind, the AFM subsystems are optimized including a buzzer-based multi-actuated scanner, custom driving and demodulation circuits for tapping mode operation, and AFM control algorithm implementation on myRIO with LabVIEW. The performance of the system is verified with imaging of calibration gratings. For future works, the graduate-level course developed for precision mechatronics will be offered to obtain feedback from the students to optimize the design and the course. Augmentation of the low-cost AFM design for investigation of other imaging modes is also an interesting direction to pursue.

CRediT authorship contribution statement

Fangzhou Xia: Conceptualization, Methodology, Software, Validation, Formal analysis, Investigation, Resources, Data curation, Writing - original draft, Writing - review & editing, Visualization. **James Quigley:** Methodology, Software, Validation, Investigation. **Xiaotong Zhang:** Methodology, Software, Validation, Investigation. **Chen Yang:** Conceptualization, Methodology, Resources. **Yi Wang:** Conceptualization, Resources, Project administration. **Kamal Youcef-Toumi:** Writing - review & editing, Supervision, Funding acquisition.

Declaration of competing interest

The authors declare that they have no known competing financial interests or personal relationships that could have appeared to influence the work reported in this paper.

References

[1] Ju Long, Shi Zhiwen, Nair Nityan, Lv Yinchuan, Jin Chenhao, Velasco Jr Jairo, et al. Topological valley transport at bilayer graphene domain walls. Nature 2015;520(7549):650–5.

[2] Bozchalooi Iman Soltani, Houck Andrew Careaga, AlGhamdi Jwaher M, Youcef-Toumi Kamal. Design and control of multi-actuated atomic force microscope for large-range and high-speed imaging. Ultramicroscopy 2016;160:213–24.

[3] Ando Toshio. Filming dynamic processes of proteins by high-speed AFM. Biophys J 2013;104(2, Suppl. 1):386a.

[4] Yang Chen, Xia Fangzhou, Wang Yi, Truncale Stephen, Youcef-Toumi Kamal. Design and control of a multi-actuated nanopositioning stage with stacked structure. In: 2019 American control conference. IEEE; 2019, p. 3782–8.

[5] Yong YK, Moheimani SOR, Kenton BJ, Leang KK. Invited review article: High-speed flexure-guided nanopositioning: Mechanical design and control issues. Rev Sci Instrum 2012;83(12):121101.

[6] Yang Chen, Li Changle, Xia Fangzhou, Zhu Yanhe, Zhao Jie, Youcef-Toumi Kamal. Charge controller with decoupled and self-compensating configurations for linear operation of piezoelectric actuators in a wide bandwidth. IEEE Trans Ind Electron 2018;66(7):5392–402.

[7] Xia F, Yang C, Wang Y, Youcef-Toumi K. Bandwidth based repetitive controller design for a modular multi-actuated AFM scanner. In: 2019 American control conference; 2019, p. 3776–81.

[8] Reifenberger Ron, Raman Arvind. ME 597/PHYS 570: Fundamentals of atomic force microscopy (Fall 2010). 2010.

[9] Wang Wei-Min, Huang Kuang-Yuh, Huang Hsuan-Fu, Hwang Shouh, Hwu En-Te. Low-voltage and high-performance buzzer-scanner based streamlined atomic force microscope system. Nanotechnology 2013;24(45):455503.

[10] Amin-Shahidi Darya, Trumper David. Macro-scale atomic force microscope: An experimental platform for teaching precision mechatronics. Mechatronics 2015;31:234–42.

[11] Asakawa Hitoshi, Fukuma Takeshi. Spurious-free cantilever excitation in liquid by piezoactuator with flexure drive mechanism. Rev Sci Instrum 2009;80(10):103703.

[12] Xia Fangzhou, Yang Chen, Wang Yi, Youcef-Toumi Kamal, Reuter Christoph, Ivanov Tzvetan, et al. Lights out! nano-scale topography imaging of sample surface in opaque liquid environments with coated active cantilever probes. Nanomaterials 2019;9(7):1013.

[13] Holz Mathias, Guliyev Elshad, Ahmad Ahmad, Ivanov Tzvetan, Reum Alexander, Hofmann Martin, et al. Field-emission scanning probe lithography tool for 150mm wafer. J Vacuum Sci Technol B 2018;36(6):06JL06.

[14] Ahmad Ahmad, Ivanov Tzvetan, Angelov Tihomir, Rangelow Ivo W. Fast atomic force microscopy with self-transduced, self-sensing cantilever. J Micro/Nanolithogr MEMS MOEMS 2015;14(3):1–8.

[15] Holz Mathias, Reuter Christoph, Ahmad Ahmad, Reum Alexander, Ivanov Tzvetan, Guliyev Elshad, et al. Parallel active cantilever AFM tool for high-throughput inspection and metrology. In: Ukraintsev Vladimir A, Adan Ofer, editors. Metrology, inspection, and process control for microlithography XXXIII, vol. 10959. International Society for Optics and Photonics, SPIE; 2019, p. 444–9.

[16] Rangelow Ivo W, Ivanov Tzvetan, Ahmad Ahmad, Kaestner Marcus, Lenk Claudia, Bozchalooi Iman S, et al. Review article: Active scanning probes: A versatile toolkit for fast imaging and emerging nanofabrication. J Vacuum Sci Technol B 2017;35(6):06G101.

[17] Lavrik Nickolay V, Sepaniak Michael J, Datskos Panos G. Cantilever transducers as a platform for chemical and biological sensors. Rev Sci Instrum 2004;75(7):2229–53.

[18] Gotszalk Teodor, Rangelow Ivo W, Dumania Piotr, Grabiec Piotr B. Cantilever with integrated wheatstone bridge piezoresistive deflection sensor: analysis of force interaction measurement sensitivity. In: Microlithography and metrology in micromachining II, vol. 2880. International Society for Optics and Photonics; 1996, p. 264–71.

[19] Ivanov Tzv, Gotszalk T, Grabiec P, Tomerov E, Rangelow IW. Thermally driven micromechanical beam with piezoresistive deflection readout. Microelectron Eng 2003;67:550–6.

[20] Giessibl Franz J. The qPlus sensor, a powerful core for the atomic force microscope. Rev Sci Instrum 2019;90(1):011101.

[21] Wu Zhichao, Guo Tong, Tao Ran, Liu Leihua, Chen Jinping, Fu Xing, et al. A unique self-sensing, self-actuating AFM probe at higher eigenmodes. Sensors 2015;15(11):28764–71.

[22] Beaulieu LY, Godin Michel, Laroche Olivier, Tabard-Cossa Vincent, Grütter Peter. A complete analysis of the laser beam deflection systems used in cantilever-based systems. Ultramicroscopy 2007;107(4–5):422–30.

[23] Hwu Edwin En-Te, Boisen Anja. Hacking CD/DVD/blu-ray for biosensing. ACS Sensors 2018;3(7):1222–32.

[24] Labuda Aleksander, Proksch Roger. Quantitative measurements of electromechanical response with a combined optical beam and interferometric atomic force microscope. Appl Phys Lett 2015;106(25):253103.

[25] Manalis SR, Minne SC, Atalar Abdullah, Quate CF. Interdigital cantilevers for atomic force microscopy. Appl Phys Lett 1996;69(25):3944–6.

[26] Michels T, Rangelow IW, Aksyuk V. Cantilever array with optomechanical readout and integrated actuation for simultaneous high sensitivity force detection. In: 2016 international conference on optical MEMS and nanophotonics; 2016, p. 1–2.

[27] Dukic Maja, Adams Jonathan D, Fantner Georg E. Piezoresistive AFM cantilevers surpassing standard optical beam deflection in low noise topography imaging. Sci Rep 2015;5:16393.

[28] Yamanaka Kazushi, Nakano Shizuka. Ultrasonic atomic force microscope with overtone excitation of cantilever. Japanese J Appl Phys 1996;35(6S):3787.

[29] Inada Natsumi, Asakawa Hitoshi, Kobayashi Taiki, Fukuma Takeshi. Efficiency improvement in the cantilever photothermal excitation method using a photothermal conversion layer. Beilstein J Nanotechnol 2016;7(1):409–17.

[30] Sarov Y, Ivanov T, Frank A, Rangelow IW. Thermally driven multi-layer actuator for 2D cantilever arrays. Appl Phys A 2011;102(1):61–8.

[31] Jayanth GR, Jhiang Sissy M, Menq Chia-Hsiang. Two-axis probing system for atomic force microscopy. Rev Sci Instrum 2008;79(2):023705.

[32] Desbiolles Benoit XE, Furlan Gabriela, Schwartzberg Adam M, Ashby Paul D, Ziegler Dominik. Electrostatically actuated encased cantilevers. Beilstein J. Nanotechnol 2018;9(1):1381–9.

[33] Long Christian J, Cannara Rachel J. Modular apparatus for electrostatic actuation of common atomic force microscope cantilevers. Rev Sci Instrum 2015;86(7):073703.

[34] Ruppert Michael G, Harcombe David M, Ragazzon Michael RP, Moheimani SO Reza, Fleming Andrew J. A review of demodulation techniques for amplitude-modulation atomic force microscopy. Beilstein J Nanotechnol 2017;8(1):1407–26.

Fangzhou Xia received his M.S. and Ph.D. degrees in Mechanical Engineering from Massachusetts Institute of Technology (MIT), US, in 2017 and 2020. He obtained his dual bachelor degrees in Mechanical Engineering from University of Michigan, Ann Arbor, US, and in Electrical and Computer Engineering from Shanghai Jiao Tong University, China, in 2015. He is a Postdoctoral Research Associate in the Mechatronics Research Lab and teaching assistant for the introduction to robotics class at MIT. His is interested in the field of control, robotics and instrumentation with application in precision mechatronic systems, microscopy and learning-based motion control.

James Quigley served as a human intelligence collector sergeant in the US army between 2007 to 2015 and studied Electrical and Electronics Engineering in Monterey Peninsula College between 2015 and 2017. He is currently an undergraduate student in the Electrical Engineering and Computer Science department at the Massachusetts Institute of Technology (MIT). His research interest is in the design of power systems, signal processing circuits and nanoelectronics.

Xiaotong Zhang received his M.S. degree in Mechanical Engineering from Massachusetts Institute of Technology (MIT), US, in 2019. He obtained his bachelor degree in Naval Architecture and Ocean Engineering from Shanghai Jiao Tong University, China, in 2017. He is currently a Ph.D. candidate in the Mechanical Engineering department at MIT working in the Mechatronics Research Lab. His research interests include robotic system, computational fluid dynamics for in-pipe power generator design, and learning methods for large scale logistic system optimization.

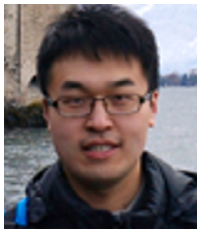

Chen Yang received the B.S., M.S. and Ph.D. degrees from the School of Mechatronics Engineering, Harbin Institute of Technology (HIT), Harbin, China, in 2009, 2012 and 2017, respectively. He was also a joint Ph.D. student of Swiss Federal Institute of Technology, Lausanne, Switzerland, from 2013 to 2015. Currently, he is a Postdoctoral Research Associate with the Mechanical Engineering Department, Massachusetts Institute of Technology, Cambridge, MA, USA. His research interests include design and control of high-speed atomic force microscopy, precision motion control and piezoelectric self-sensing techniques.

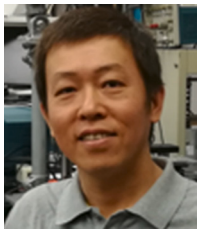

Yi Wang received the M.S. degree in Physics and Chemistry of Materials from Qingdao University of Science and Technology, China, and Ph.D. degree in Physics and Chemistry of Materials from General Research Institute for Nonferrous Metals, Beijing, China, in 2004 and 2008, respectively. From 2008 to 2010, he worked as a Postdoctoral Fellow with the Institute of Physics, Chinese Academy of Science, Beijing, in the field of condensed matter physics. In 2010, he joined Synfuels China Technology Co., Ltd., Beijing, as a Senior Engineer. Since 2017, he is with the Mechanical Engineering Department of Massachusetts Institute of Technology (MIT), Cambridge, MA, USA, as a Visiting Scientist, focusing on high-speed atomic force microscopy related research topics. His research interests include thin film growth, synthesis of nanomaterials, energy materials, techniques for characterization of nanomaterials, and precision machine design.

Kamal Youcef-Toumi (M'03) received the B.S. degree in mechanical engineering from the University of Cincinnati, Cincinnati, OH, USA, in 1979, and the M.S. and Sc.D. degrees in mechanical engineering from the Massachusetts Institute of Technology (MIT), Cambridge, MA, USA, in 1981 and 1985, respectively. He is a full Professor in the mechanical engineering department at MIT and director of the Mechatronics Research Lab. His research interests include modeling, design, instrumentation, and control systems theory and their applications to dynamic systems.